EasyChair Preprint

№ 171

Erosion Analysis of the Upstream Riverbank Slope: Pleasant Valley Dam, Bishop, California

Saddanathapillai Nesarajah, Taras Kruk, Christopher Goetz, Steven Rusak, Yongqiang Lan, Liping Yan, Cesar Larios and Steven Kehrmeyer

May 25, 2018

Erosion Analysis of the Upstream Riverbank Slope at Pleasant Valley Dam

S. Nesarajah[1], Taras B. Kruk[2], Christopher Goetz[3], Steven A. Rusak[4], Frank Lan[5], Liping Yan[6], Cesar H. Larios[7], and Steven R. Kehrmeyer[8]

[1]Principal Geotechnical Engineer, AECOM, 300 S. Grand Ave., LA, CA 90071
[2]Principal Hydrogeologist, AECOM, 1111 3rd Ave., Seattle, WA 98101
[3]Principal Engineering Geologist, AECOM, 999 Town and Country Road, Orange, CA 92868
[4]Senior Scientist, AECOM, 700 G St., Anchorage, AK 99501
[5]Principal Water Resources Engineer, AECOM, 6200 S. Quebec Street, Greenwood Village, CO 80111
[6]Technical Specialist, LADWP, 111 N. Hope St., Los Angeles, CA 90012
[7]Engineering Geologist Associate, LADWP, 111 N. Hope St., LA, CA 90012
[8]Civil Engineer, LADWP, 111 N. Hope St., Los Angeles, CA 90012

ABSTRACT: A study was conducted to evaluate ongoing erosion of the upstream riverbank slope at the Pleasant Valley Dam. There is continued erosion concerns along the western shoreline abutment and potential future damage to dam structures due to slope failure caused by erosion. The dam is composed of compacted earth fill containing a mixture of gravel, sand, and silt; and the abutments are composed of Bishop Tuff. A geotechnical and geochemical investigation was performed consisting of core rock sampling, bulk sampling, and reservoir water sample testing. Geotechnical, geochemical, and wave runup and wind setup analyses were performed to provide mitigation recommendations. Geochemical analyses indicated that chemical dissolution of the earth materials is insignificant, and that clay swelling is also not a factor. The wave runup and wind setup analyses simulated wave action and erosive forces; indicating wave heights of 1.5 to 1.8 feet and strength testing along this zone did not indicate weakened rock. The freeze thaw mechanical weathering is considered one of primary causes for the erosion. The overall results indicate that mitigation should focus on controlling sequential wetting and drying near the air-water interface, and/or limit the penetration of water in the erosion area to avoid mechanical weathering.

INTRODUCTION

Pleasant Valley Dam is located in Inyo County, near the lower end of the Owen's River Gorge, approximately 8 miles northwest of Bishop, California, USA (Figure 1). The dam functions to maintain the Pleasant Valley Reservoir, a freshwater reservoir

of approximately 3,825 acre-feet. Built from 1954 to 1956, the dam is composed of compacted earth fill, which was constructed using the same borrow material for both its pervious and impervious zones (LADWP 1982). Both the pervious and impervious zones are composed of a mixture of gravel, sand and silt derived from a borrow site located approximately 1.2 miles to the south. Native material consists of Bishop Tuff, and lesser amounts of ash associated with the Bishop Tuff.

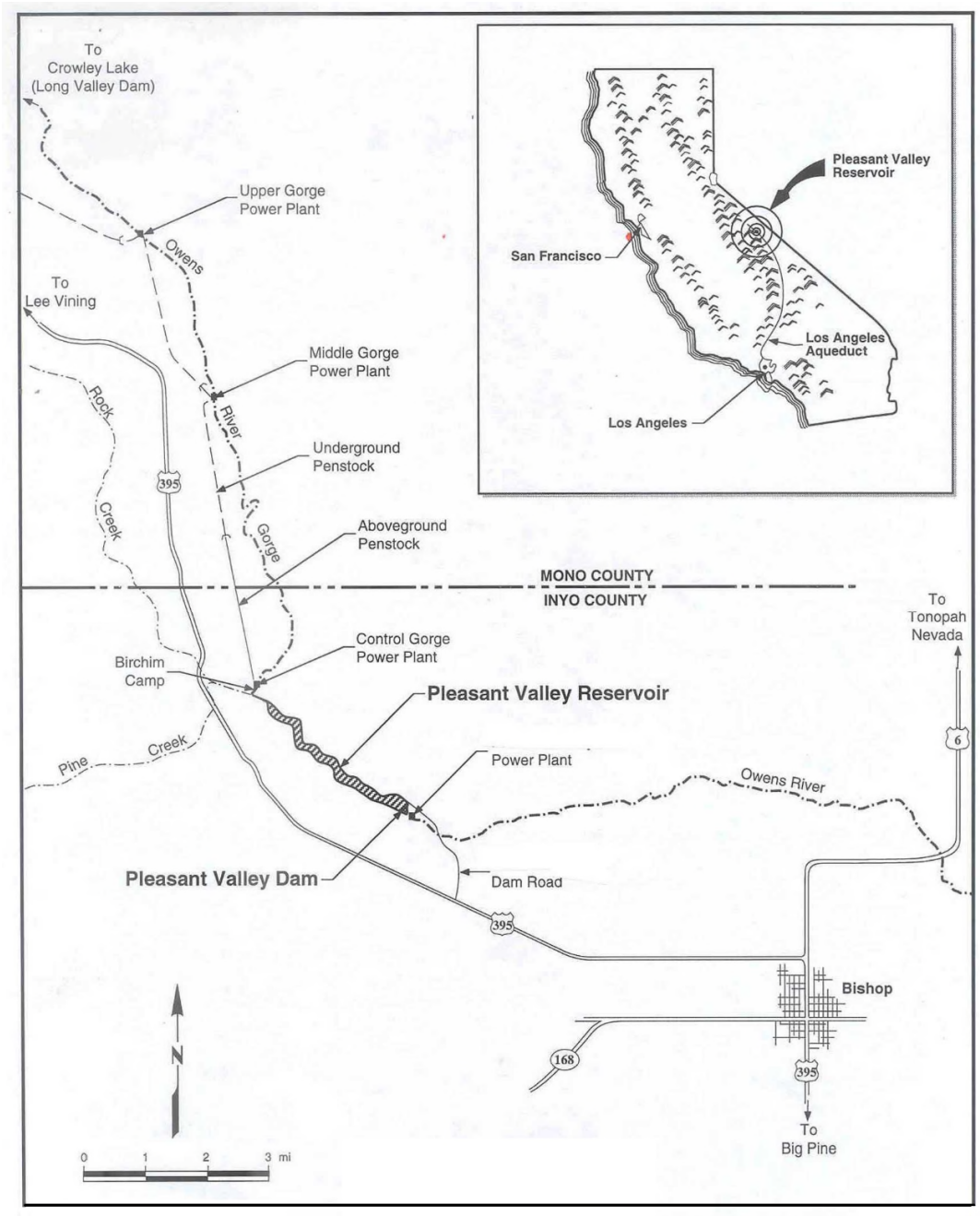

FIG. 1. Site vicinity map.

The maximum reservoir level has been maintained at 8 feet below the spillway, at Elevation 4,390 feet or lower following the 1971 San Fernando earthquake and

subsequent seismic-stability evaluations (LADWP 1980; Dames & Moore 1985). The results of a more recent seismic-stability analysis of the embankment using newly developed data for the streambed deposits indicated that operating at full reservoir capacity may be feasible (URS 2001).

The scope of work included geochemical analysis of the Bishop Tuff and of the reservoir water to determine if potential chemical reactions are occurring. A wave runup and wind setup analysis was performed to estimate freeboard limits where materials are exposed to erosion. A slope stability analysis was performed to assess the potential for erosion-induced slope movements or rock falls, and to provide mitigation recommendations to help prevent further erosion of the right side (western) abutment. Detailed descriptions and supporting materials are included in a *Geotechnical Investigation Report* (URS 2017). Presented herein are the results of an assessment for the nature and rate of ongoing erosion of the upstream riverbank slope of the Pleasant Valley Dam.

INVESTIGATION AND ANALYSIS

Geochemical and Geotechnical Analysis

Sample Collection and Analysis

As part of this investigation, exploratory cores were conducted at six locations (PVD-1 through PVD-6) that represent areas of interest along the left and right abutments potentially affected by chemical weathering (Figure 2). Samples collected from locations PVD-2 to PVD-6 ranged from elevation 4388 to 4390 feet Mean Sea Level (MSL) with 4390 being the reservoir's current maximum normal operating level surface. Samples were collected from location PVD-1 at just above the previous maximum normal operating level surface of 4399 feet MSL. In addition, a block sample was collected from the exposure just above the reservoir high water level near cores PVD-3 and PVD-4. The sample collection procedures and field descriptions for are described in Appendix A of the *Geotechnical Investigation Report* (URS 2017).

A total of 15 representative soil samples (PVD-1-1, PVD-1-2, PVD-1-3, PVD-1-4, PVD-1-5, PVD-2-1, PVD-2-2, PVD-3-1, PVD-3-2, PVD-5A-2, PVD-5A-5, PVD-5B-1, PVD-5B-2, PVD-6A-1 and PVD-6A-2) and two water samples (PVD-W-1 and PVD-W-2) were submitted for geochemical analysis. At each sample location "1-1" represents an initial shallow sample and "1-2" is the deeper sample. The "A" is an initial core location and "B" is a second adjacent core location. For purposes of this study, the rock samples and the water samples were analyzed for minor and trace constituents (EPA Method 200.7) and paste pH (EPA-600/2-78-054). The block sample collected from the exposure at PVD-3/PVD-4 was tested for gradation of soils with water content (ASTM D1140 and D2216), Atterberg Limits (ASTM D 4318), and swell/collapse (ASTM D 4546). A copy of the laboratory reports is included in Appendix B of the *Geotechnical Investigation Report* (URS 2017). Results of the rock sample geochemical analyses, the water sample analyses, and the strength testing of the core samples are summarized in Tables 1 through 4.

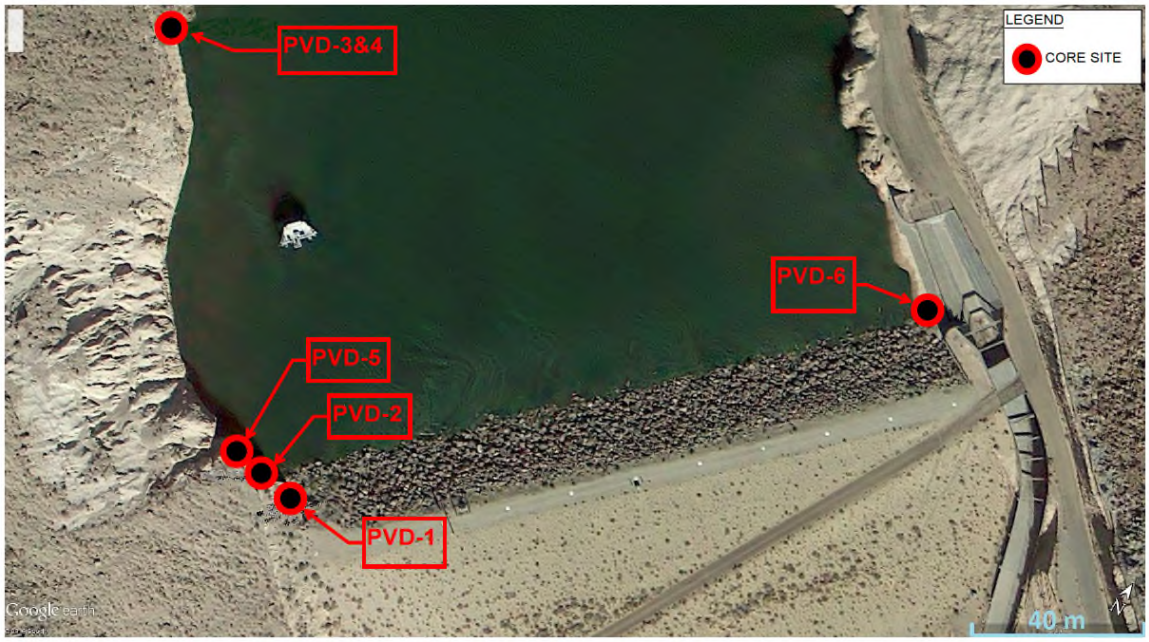

FIG. 2. Sample core location map.

At locations PVD-1 and PVD-2, concentrations of iron, aluminum, and zinc, were generally lower in the samples collected near the surface relative to those at depth, suggesting that some redistribution of iron, aluminum and zinc may be occurring because of chemical weathering reactions at the face of the right abutment.

In addition, concentrations of calcium were relatively lower in the sample collected near the surface at PVD-1 relative to samples collected from deeper depths, suggesting that dissolution of calcite minerals may have historically occurred near the rock/ water interface.

The water can generally be described as relatively soft, with low concentrations of calcium (19.5 to 20.4 mg/L) and magnesium (6.19 to 6.29 mg/L), basic pH (pH = 8.59), and moderate buffering capacity (alkalinity = 149 mg/L as CaCO3).

Due to the basic pH of the water, aqueous concentrations of transition metals such as cadmium, chromium, cobalt, copper, lead, nickel, zinc, and iron were below detection limits for the analysis because these metals are present primarily as oxidized species with low solubility at the elevated pH values observed in the reservoir water.

Results of the block sample testing indicated 55.4% passing a #4 sieve, 36.5% passing a #100 sieve, and 24.3% passing a #200 sieve. The Atterberg limits indicated that the material, classified as “Pink Tuff,” had a Plasticity Index and Liquid Limit of near zero. The swell/collapse test indicated a swell strain of 0.1%.

Interpretation of Results

Previous research suggests the Bishop Tuff is a high-silica rhyolite that was emplaced ~ 0.7 million years ago during collapse of the Long Valley caldera and consists of erupted material representing a range of cooling histories and volatile contents. The tuff is made up of a basal ash-fall pumice deposit and five major ash-flow tuff emplacements (Skirius et al. 1990).

Table 1. Composition and Paste pH of Solid Phase Samples PVD 1-1 – PVD 2-2

SAMPLE	PVD 1-1	PVD 1-2	PVD 1-3	PVD 1-4	PVD 1-5	PVD 2-1	PVD 2-2
Antimony (mg/kg)	ND	ND	ND	ND	ND	ND	ND
Arsenic (mg/kg)	ND	ND	ND	ND	ND	ND	ND
Barium (mg/kg)	1.96	2.75	3.21	5.60	5.50	2.51	2.52
Cadmium (mg/kg)	ND	ND	ND	ND	ND	ND	ND
Chromium (mg/kg)	ND	ND	ND	ND	ND	ND	ND
Cobalt (mg/kg)	758	629	447	525	515	184	179
Copper (mg/kg)	12.1	10.7	7.89	13.8	13.2	3.22	6.01
Lead (mg/kg)	ND	ND	0.877	0.697	0.616	0.703	0.822
Molybdenum (mg/kg)	ND	ND	ND	ND	ND	ND	ND
Nickel (mg/kg)	0.451	0.526	0.448	0.497	0.391	ND	0.316
Selenium (mg/kg)	ND	ND	ND	ND	ND	0.768	ND
Zinc (mg/kg)	4.11	4.39	5.21	4.28	3.99	3.01	5.88
Aluminum (mg/kg)	925	1350	1510	1380	1210	938	1230
Calcium (mg/kg)	381	612	663	647	584	540	382
Iron (mg/kg)	828	1300	1620	2050	1410	766	1220
Magnesium (mg/kg)	167	273	329	251	224	253	264
Manganese (mg/kg)	21.9	30.5	36.3	32.1	32.4	36.3	29.2
Potassium (mg/kg)	484	625	708	809	747	950	947
Sodium (mg/kg)	617	558	631	796	749	743	529
Sulfate (mg/kg)	ND	ND	ND	11	11	22	ND
Alkalinity (mg/kg)	100	75	65	55	60	75	70
paste pH	9.32	9.30	9.03	8.71	8.62	9.32	8.89

The pumice is primarily silicon dioxide (amorphous aluminum silicate), some aluminum oxide, and trace amounts of other oxides. In the case of the Bishop Tuff, the glass phases of the material are comprised of approximately 73.4 % to 77.9 % SiO2, 11% to 13 % Al2O3, and smaller amounts of sodium oxides and potassium oxides (Hildreth and Wilson 2007).

The primary mineral assemblage of the Bishop Tuff consists of crystals of high temperature beta-quartz, sanidine, oligoclase, biotite, orthopyroxene, clinopyroxene, palepink zircon, allanite, titanomagnetite, and ilmenite (Izett et al. 1988). Zircon, titanomagnetite, and ilmenite are invariably small, nearly complete euhedral crystals. Quartz, sanidine, oligoclase, and allanite from samples of the Bishop Tuff ash flows are generally broken crystals or cleavage fragments (Izett et al. 1988).

Due to the basic pH and moderate buffering capacity of the reservoir water, dissolution rates of the silicate minerals comprising the dam abutment are likely to be slow. The distributions of iron and calcium across depth in core samples collected from the areas of interest suggests that some iron and calcium-based minerals may be

redistributed as a result of dissolution from the surface layer.

Dissolution of rhyolite and other silicate minerals that comprise the Bishop Tuff would be very slow at the pH values measured in the reservoir water (Izett et al. 1988; Yokoyama and Banfield 2002).

The strength testing that was done for this investigation did not provide evidence to support the supposition that the rock that is near the air water interface has been weakened by dissolution or any other means. By comparing samples that were collected from various distances beneath the interface, there was no noticeable trend in the variation of the unconfined compressive strength. However, if there is a relatively thin (less than a couple of inches) dissolution rind of weakened rock at the interface then it is unlikely that the coarse sampling and testing procedures that were employed for this investigation would have isolated it to allow a characterization of its strength.

Table 2. Composition and Paste pH of Solid Phase Samples PVD 3-1 – PVD 6A-2

SAMPLE	PVD 3-1	PVD 3-2	PVD 5A-2	PVD 5A-5	PVD 5B-1	PVD 5B-2	PVD 6A-1	PVD 6A-2
Antimony (mg/kg)	ND	ND	ND	ND	ND	ND	ND	ND
Arsenic (mg/kg)	ND	ND	ND	ND	ND	ND	ND	ND
Barium (mg/kg)	2.10	1.78	1.86	1.27	1.54	1.84	4.62	4.58
Cadmium (mg/kg)	ND	ND	ND	ND	ND	ND	ND	ND
Chromium (mg/kg)	0.321	ND	ND	ND	ND	ND	ND	ND
Cobalt (mg/kg)	3.81	0.501	2.61	0.318	ND	ND	ND	ND
Copper (mg/kg)	30.1	3.07	19.8	2.34	ND	ND	ND	0.602
Lead (mg/kg)	0.635	0.724	0.808	0.564	0.642	0.668	0.575	0.565
Molybdenum (mg/kg)	ND	ND	ND	ND	ND	ND	ND	ND
Nickel (mg/kg)	0.620	ND	0.870	ND	ND	ND	ND	ND
Selenium (mg/kg)	ND	ND	ND	ND	ND	ND	ND	ND
Zinc (mg/kg)	3.67	3.28	2.95	2.16	2.14	2.95	2.71	3.66
Aluminum (mg/kg)	882	842	989	798	794	720	605	684
Calcium (mg/kg)	347	317	398	313	331	321	381	300
Iron (mg/kg)	1340	814	936	726	649	573	754	1090
Magnesium (mg/kg)	239	247	253	206	211	196	279	256
Manganese (mg/kg)	27.5	43.5	22.6	17.8	18.9	18.1	18.9	37.5
Potassium (mg/kg)	591	511	466	322	393	388	540	549
Sodium (mg/kg)	435	346	473	304	380	402	296	336
paste pH	7.61	N/A	7.66	7.61	7.45	7.58	7.83	N/A

Table 3. Composition and pH of Water Samples PVD-W-1 and PVD-W-2

SAMPLE	PVD W-1	PVD W-2
Antimony (mg/L)	ND	ND
Arsenic (mg/L)	0.0829	0.0778
Barium (mg/L)	0.0209	0.0212
Cadmium (mg/L)	ND	ND
Chromium (mg/L)	ND	ND
Cobalt (mg/L)	ND	ND
Copper (mg/L)	ND	ND
Lead (mg/L)	ND	ND
Molybdenum (mg/L)	ND	ND
Nickel (mg/L)	ND	ND
Selenium (mg/L)	ND	ND
Zinc (mg/L)	ND	ND
Aluminum (mg/L)	ND	ND
Calcium (mg/L)	20.4	19.5
Iron (mg/L)	ND	ND
Magnesium (mg/L)	6.29	6.19
Manganese (mg/L)	0.0156	0.0213
Potassium (mg/L)	6.34	6.24
Sodium (mg/L)	67.2	64.4
Sulfate (mg/L)	18	200
Alkalinity (mg/L)	149	N/A
pH	8.59	1.63*

* = outlier and not representative of reservoir water.

Rather than dissolution of the rock, an alternative explanation for increased erosion at reservoir levels is that rock saturated by reservoir water during the winter season could be undergoing mechanical weathering by the process of ice wedging. When fresh water freezes, it increases in volume by about 9% and the effect of this expansion can cause ice wedging of the rock (Walder et al. 1986). During the field investigation it was noticed that the Bishop Tuff rock at reservoir levels near the right abutment characteristically exhibits a zone of surface parallel fracturing that extends beneath the rock surface for approximately 1-2 inches. It seems plausible that reservoir water could infiltrate these narrow, near surface cracks, subsequently freeze, and the expansion causes a spall or flake of the rock material to break off. This process could potentially repeat itself on a daily interval when above freezing temperatures occur during the day and sub-freezing temperatures occur at night.

Table 4. Unconfined Compressive Strength

SAMPLE	APPROXIMATE ELEVATION OF SAMPLE (FEET)	DEPTH BELOW SURFACE (INCHES)	TEST	COMPRESSIVE STRENGTH (MPA)
Bulk Sample at PVD-1	4400	0-10	UCS	0.6
Bulk Sample at PVD-2	4389	0-10	UCS	0.3
PVD-3B-1	4392	0-3	PL	0.8
PVD-4B-1	4392	0-6	PL	1.0
PVD-5A-1	4389	1.5-6	PL	1.0
PVD-5B-3	4389	12-16	PL	1.0
PVD-5B-4	4389	16-18	PL	0.8
PVD-5D-1	4389	7-9	PL	0.8
PVD-5D-2	4389	10-14	PL	0.8
PVD-5D-3	4389	15-20	UCS	0.3
PVD-6A-3	4388	7-9	PL	1.6
PVD-6A-4	4388	9-14	PL	0.8
PVD-6A-5	4388	14-18	PL	0.8
PVD-6B-1	4388	1-6	PL	0.8
PVD-6B-2	4388	10-15	PL, UCS	1.0, 0.4

Wave Runup and Wave Setup Analysis

The wave runup and setup analysis was generated based on the Pleasant Valley Dam geometry and climatic wind data obtained from the National Oceanic and Atmospheric Administration (NOAA 2017). The analysis was used to determine the wind-generated wave height, wave set-up, and run-up for the dam. Relevant worksheets and calculation outputs are included in Appendix E of the *Geotechnical Investigation Report* (URS 2017).

Technical Analysis

The analysis followed guidelines/calculations prepared by the United States Department of Agriculture (USDA 1983) and United States Department of the Interior Bureau of Reclamation (USBR 1992). The procedures included three steps and are described below.

Step 1 - Estimate the Reservoir Fetch Length: In accordance with USDA TR-69 guidelines (USDA 1983), reservoir fetch length was calculated with radials at 6 degree spacing. The location of the radials was adjusted along the face of the dam so that the maximum average fetch length could be estimated. Figure 3 shows the radials used for calculating the maximum average fetch length. The maximum

average fetch length was calculated to be 0.29 miles at the left side of the dam embankment, and it is 0.2 miles at the right side of the dam embankment.

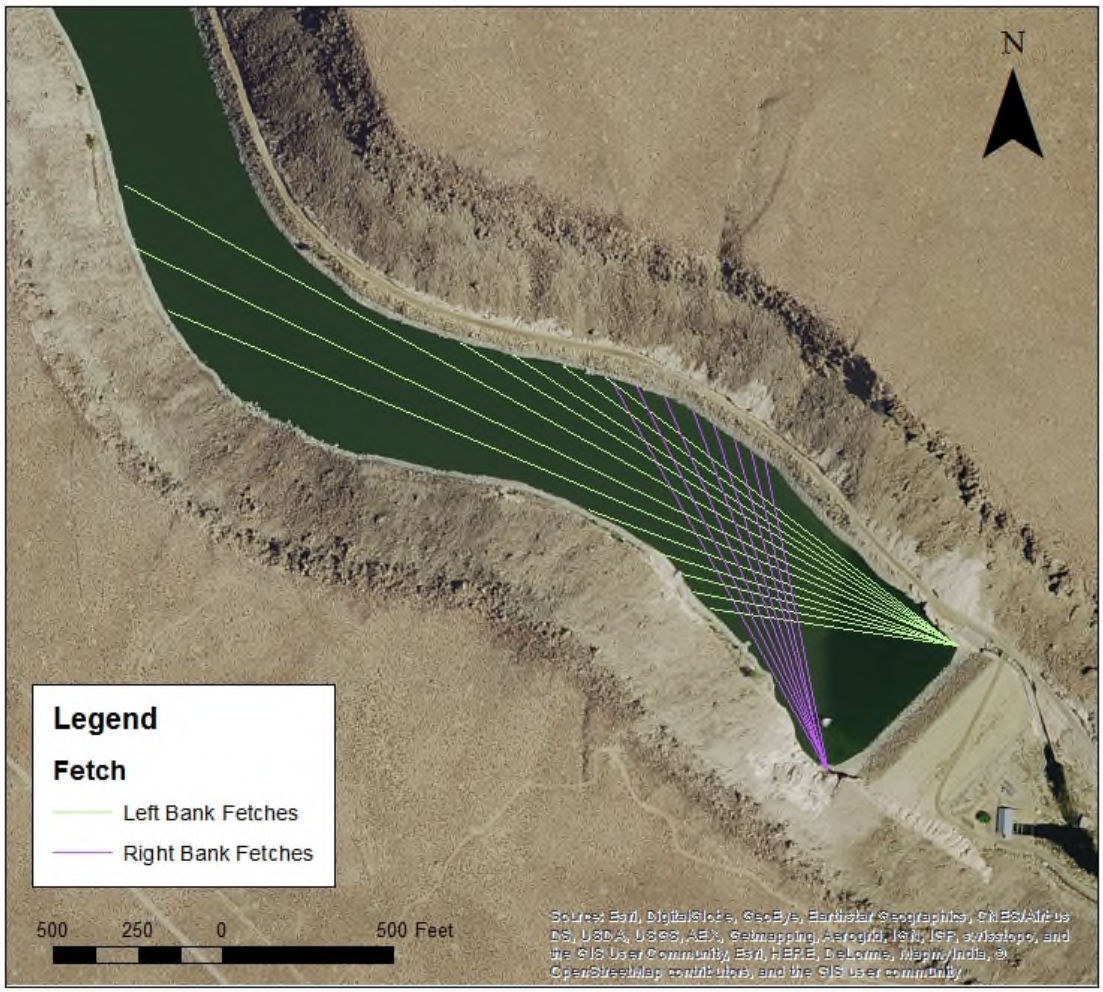

FIG. 3. Work map of the wind fetch length computation.

Step 2 - Estimate the Peak Gust Wind Velocity: The maximum wind gust speed was obtained from NOAA climatic wind data (NOAA 2017). In the State of California, the maximum wind speed is found to be 85 mph (URS 2017). This wind speed was subsequently adopted for determining the wind actions in this calculation.

In general, longer fetch and faster wind speed produce higher waves. Sustained maximum wind speed over a certain period is the key to determine the wave height. The sustained maximum average wind speed decreases as the corresponding duration increases. The relationship between overland wind speed and duration corresponding to the fastest mile wind is specified in Figure 5 of USDA TR-69 and summarized in Table 5.

The generalized maximum wind speeds and durations were plotted as the red curve (connecting diamond symbols) in Figures 4 and 5 for the left and right banks, respectively.

Table 5. Maximum Wind Speed Relationship

FASTEST MILE WIND SPEED (MPH)	RATIO OF LAND WIND SPEED TO THE FASTEST MILE WIND SPEED FOR THE DURATIONS		
	30 MIN	60 MIN	100 MIN
100	52%	46%	41%
80	57%	51%	47%
60	65%	59%	55%

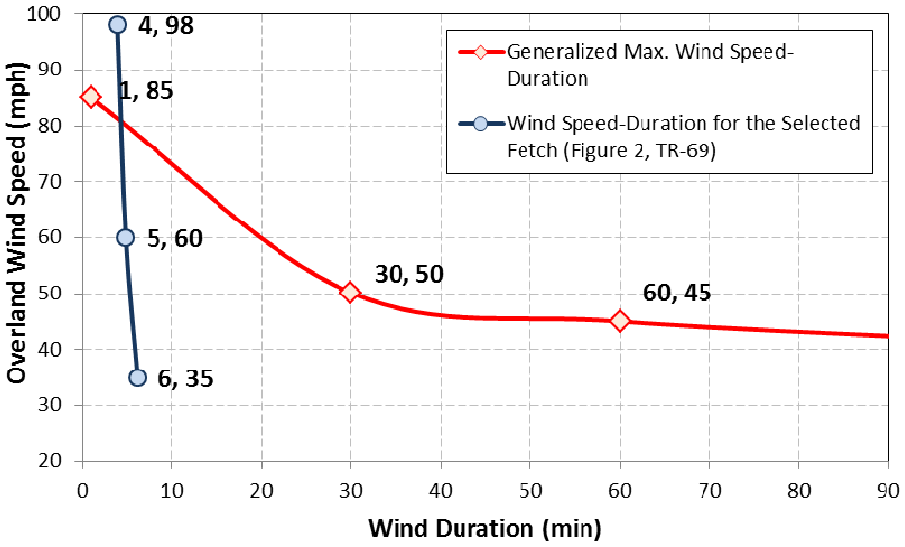

FIG. 4. Plot of wind speed vs duration (left bank).

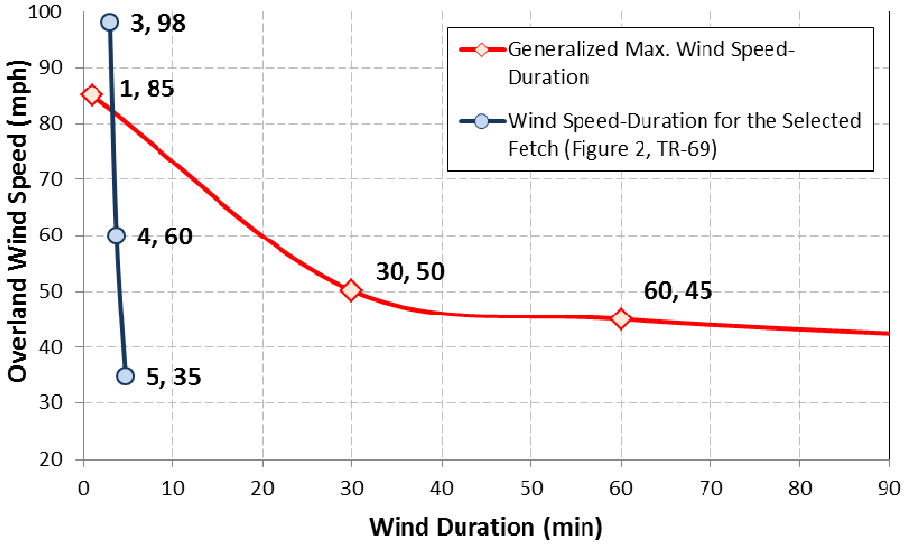

FIG. 5. Plot of wind speed vs duration (right bank).

For the selected effective fetch, wave duration is related to the overland wind speed as described in the following empirical relationship (USDA 1983).

$$g\frac{T}{U_L} = 27.99\left(\frac{g \cdot F_e}{{U_L}^2}\right)^{0.72} \quad (1)$$

where U_L = overland wind speed in ft/sec; g = gravity acceleration (32.2 ft/sec^2); T = wave duration in seconds, herein it means the minimum wind duration required for generation of wave heights for a corresponding effective fetch and wind speed; F_e = site specific effective fetch in feet.

The blue lines (connecting circle symbols) in Figures 4 and 5 represent the relationship for the effective fetch selected. The intersection of these two curves agrees with the generalized maximum wind characteristics and the effective fetch and produces the worst condition that generates the maximum wave height. The overland wind speeds of 82 mph and 83 mph were defined as the design wind speeds for the left and right banks, respectively. These design wind speeds were used to estimate wind set-up, wave height, and run-up herein.

The NOAA overland wind speed was measured at 25 ft above ground. Because of smoother and more uniform surface conditions, overwater wind speeds, U_w, are generally higher than overland speeds. The following equation is used to calculate the overwater wind speed (USDA 1983).

$$U_w = \beta \cdot U_L \quad (2)$$

where β = wind speed adjustment factor, shown in Figure 6 (USDA 1983).

According to Figure 6, β was interpolated as 1.1 for the effective fetch length. Then, the adjusted overwater wind speed is about 91 mph for both sides.

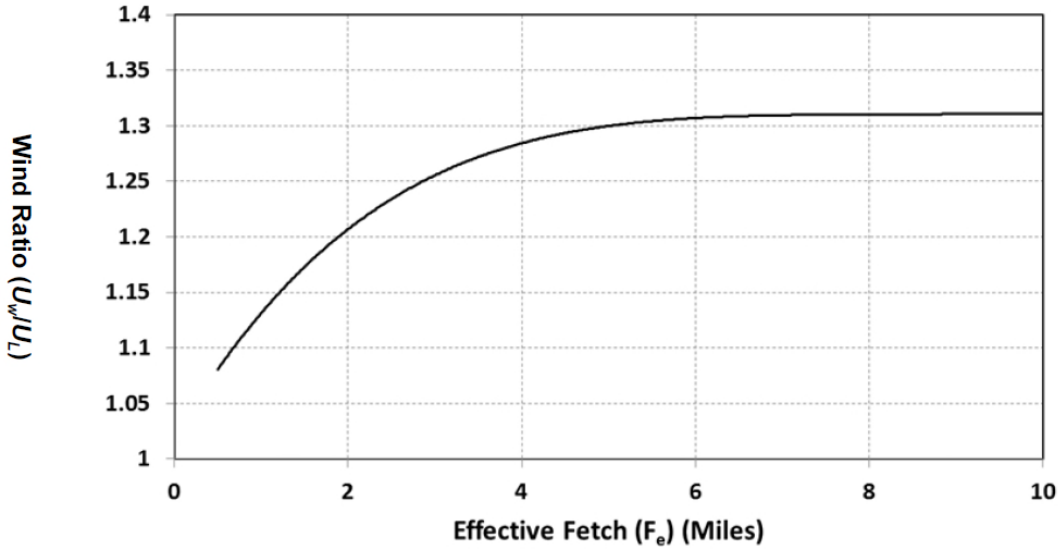

FIG. 6. Wind speed relationship – water to land (USDA 1983).

Step 3 - Calculate the Wave Run-up and the Wind Set-up: The wave set-up was calculated using the USBR (1992) equation shown below.

$$S = \frac{V^2 F}{1400 D} \tag{3}$$

where S = wave set-up in ft; V = wind velocity in mph; F = fetch length in miles (approximately equal to F_e); D = average water depth in ft.

The average water depth (D) was estimated based on the 1955 as-built drawings and is about 50 feet. The wave set-up was, then, computed to be about 0.02 ft and 0.03 ft for the left and right banks, respectively.

In order to calculate the wave run-up, the height of the significant wave and the wave length must first be estimated. The significant wave height can be estimated using the following equation in USDA TR-69 (USDA 1983), assuming that the effective fetch is perpendicular to the embankment:

$$g\frac{H_s}{U_L^2} = 0.0026\left(\frac{g \cdot F_e}{U_L^2}\right)^{0.47} \tag{4}$$

where H_s = significant wave height in ft.

The significant wave height was calculated to be 2.1 ft and 1.8 ft for the left and right banks, respectively.

The wave length was calculated using the USDA TR-69 (USDA 1983) equation shown below.

$$g\frac{\sqrt{L}}{U_L} = 1.041\left(\frac{g \cdot F_e}{U_L{}^2}\right)^{0.28} \quad (5)$$

where L = wave length in ft.

The significant wave length was calculated to be 30 ft and 25 ft for the left and right banks, respectively.

Interpretation of Results

The methodology of USBR ACER TM-2 (USBR 1992) was used to compute the wave run-up height, R, on the abutment bedrock. The total height of wave set-up and run-up is then computed to be 1.8 ft and 1.5 ft for the left and right banks, respectively.

SLOPE STABILITY ANALYSIS

To assess the potential for erosion-induced slope movements or rock falls, slope stability analyses were performed considering two scenarios: the current configuration with roughly 5-feet of overhang, and estimated conditions after 100 years of erosion with roughly 11 feet of overhang. Rock shear strength properties were estimated using the Hoek-Brown methodology, based on measured values of the Unconfined Compressive Strength (UCS) and reported rock mass conditions. Details of the analysis are presented in Appendix D of the *Geotechnical Investigation Report* (URS 2017).

The results indicate that the computed factor of safety for global stability for existing conditions is 1.70. For the 100 year erosion case, the computed factor of safety is only slightly lower, 1.69. Thus, the predicted erosion has little effect on the overall global stability of the slope. However, this degree of erosion would be expected to cause local rock falls and local shallow sloughing, with surficial slope movements eventually propagating upslope.

CONCLUSIONS

Examination of the strength testing and chemical composition of the solid phase materials and the chemical composition of the reservoir water suggests that chemical dissolution of the solid phase materials plays only a minor role in the ongoing erosion of the upstream riverbank slope. Furthermore, testing of the block sample at PVD-3/PVD-4 indicates that the swelling of clay minerals in the presence of water (hydric dilatation) (Wedekind et al. 2013) is not a factor. Considering the climate conditions, however, freeze/thaw may be contributing to erosion. As moisture enters the rock, freeze-thaw cycles near/during the winter season can result in mechanical weathering as water freezes, which increase its volume by up to nine percent resulting in the process of ice wedging. This supposition is supported by the field observation that a 1-2 inch wide zone of surface parallel fractures and thin spalls (flakes) of semi-dislodged rock are common in the erosion area near the right abutment.

The strength testing done in this study did not reveal the occurrence of a rind of

weakened rock near the air water interface. However, if there is a relatively narrow rind (two to three inches) it would not have been detected by the coarse sampling and testing that was done for this study.

Results of the slope stability analysis indicated that the computed factor of safety for global stability for existing conditions is 1.70 and for the 100 year erosion case is 1.69. Based on these results, the predicted erosion has little effect on the overall global stability of the slope. However, this degree of erosion would be expected to cause local rock falls and local shallow sloughing.

Mitigation should focus on controlling sequential wetting and drying of materials in the active erosion zone near the air-water interface, and/or limiting the penetration of water into the dam materials in the area of interest to avoid mechanical weathering. This could be accomplished by managing reservoir levels to prevent sequential wetting and drying in the areas of interest. Based on the wave setup and runup analysis, the air-water interface should incorporate a minimum of two feet above the upper reservoir level.

REFERENCES

Dames & Moore (1985). "Evaluation of earthquake-induced deformations of Pleasant valley dam for the LADWP." Job No. 00138-015-02, May 24.

Hildreth, W. and Wilson, C.J.N. (2007). "Compositional zoning of the Bishop tuff." *Journal of Petrology*. 48 (5): 951-999.

Izett, G.A., Obradovich, J.D. and Mehnert, H.H. (1988). "The Bishop ash bed (middle Pleistocene) and some older (Pliocene and Pleistocene) chemically and mineralogically similar ash beds in California, Nevada, and Utah." *US Geological Survey* Bulletin 1675, 37pp.

LADWP (1980). "Pleasant valley dam stability evaluation." City of Los Angeles Department of Water and Power; Power Design and Construction Division. June.

LADWP (1982). "Pleasant valley dam, alternatives to improve seismic stability." City of Los Angeles Department of Water and Power; Power System Design and Construction Division. November.

National Oceanic and Atmospheric Administration (NOAA 2017). "Climatic wind data for the United States." <*http://www.ncdc.noaa.gov/oa/climate/online/ccd/maxwind.html*>. Data through 2002.

Ruedrich, J., Kirchner, D. and Siegesmund, S. (2011). "Physical weathering of building stones induced by freeze-thaw action: a laboratory long-term study." *Environmental Earth Sciences*. 63: 1573-1586.

Skirius, C.M., Peterson, J.W., and Anderson, A.T. (1990). "Homogenizing rhyolitic glass inclusions from the Bishop tuff." *American Mineralogist*. 75: 1381-1398.

United States Department of the Agriculture (USDA 1983). "Riprap for slope protection against wave action." *Technical Release No. 69*.

United States Department of the Interior Bureau of Reclamation (USBR1992). "Freeboard criteria and guidelines for computing freeboard allowances for storage dams." *ACER Technical Memorandum No. 2. Original 1981; Revised 1992*.

URS (2001). “Re-evaluation of seismic performance and safe operating reservoir level of Pleasant valley dam for Los Angeles Department of Water and Power.” Job No. 59-00112033.01, November 16.

URS (2017). “Erosion assessment: geochemistry, strength testing and wave run-up/wave setup analysis. Pleasant Valley Dam, Bishop, CA.” *Geotechnical Investigation Report*. March 31.

Walder, J.S. and Bernard, H. (1986). "The physical weathering of frost weathering: towards a more fundamental and unified perspective". *Arctic and Alpine Research*. 8 (1): 27–32.

Wedekind, W., López-Doncel, R., Dohrmann, R., Kocher, M., and Siegesmund, S. (2013). “Weathering of volcanic tuff rocks caused by moisture expansion.” *Environmental Earth Sciences*. 69: 1203-1224.

Yokoyama,T. and Banfield, J.F. (2002). “Direct determinations of the rates of rhyolite dissolution and clay formation over 52,000 years and comparison with laboratory measurements.” *Geochimica et Cosmochimica Acta*, 66(15): 2665-2681.